# Design of Size Flexible and Leak Preventing Hydrobushing

Min Lu

***Abstract*—The success of hydromount in automotive powertrain application motivates the industry to develop the suspension bushing with the same damping generating mechanism as hydromount's: hydrobushing. The vehicle equipped with hydrobushing in the North America market was seen in late 90's. The generic problems of those early generations of hydrobushings are their size inflexibility (normally in proximity of 80 mm in diameter), and the poor reliability due to fluid leaking. This paper introduces a hydrobushing design whose inertia track is placed in the outside of an aluminum armature. Therefore the inertia track becomes independent from the main rubber element. As a result, the tri-axis static stiffness of the hydrobushing can be designed the same way as the conventional rubber bushing, resulting in flexibility in size selection. Moreover, a thin layer of rubber coated in the outside of the armature is compressed after the outer can is assembled. This compressed rubber serves as the tight sealing, along with the O-ring style design feature which is added in the armature structure, making the proposed design reliable in leak prevention. The design procedure, which involves in the determination of overall dimensions, rates and performance, is introduced based on a set of assumed criterion.**

***Index Terms*— Hydromount, Hydrobushing, Inertia track**

## I. Introduction

When oscillating fluid goes through a tube, the friction generated between the fluid and the tube surface consumes energy. In the situation of vibration, this consumed energy is the indication of damping. Two decades after General Motor Corp. was granted a patent in early 60's for a fluid generated damping device [1], the new generation of engine mount, hydromount, whose damping mechanism is based on oscillating fluid, was developed [2,3,4]. It is so successful in the isolation of vehicle vibrations that the desire for a similar device in the application of the suspension system remains strong. In late 90's, such a device, hydrobushing, was developed. The design features the carved inertia track on the plastic pieces. Those plastic pieces are molded into the main rubber element, or MRE as an abbreviation (see Fig.1 for the simplified design model). The outer can is swaged into the molded main rubber element during assembly. The swaging process, in which the outer can is pushed through a smaller diameter die, is illustrated in Fig.2. It is hoped that the inner surface of the outer can fits the curvature of the plastic pieces perfectly so the fluid does not leak when high pressured fluid flows

Manuscript received March 4, 2011; revised April 8, 2011.
Author is with Grand Valley State University, Grand Rapids, MI 49504 USA (phone: 616-331-6018; fax: 616-331-7215; e-mail: lum@gvsu.edu).

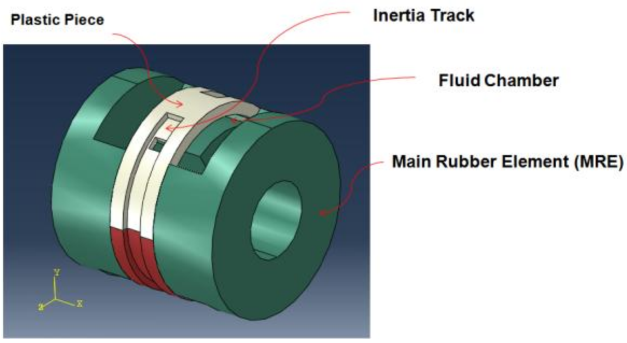


Figure 1: Typical Hydrobushing
(Inner Tube and Outer Can Omitted)

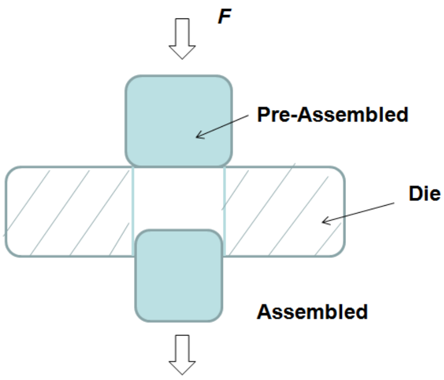


Figure 2: Out Can Swaging Process

through the inertia track. It is evident that the swaging process is not precise enough to achieve the desired outcome, which makes the design unreliable due to fluid leaking. Because the plastic pieces are molded into the main rubber element, enough rubber volume is needed to maintain its stability and enough rubber radial stiffness is needed to insure its tight fitness to the outer can inner surface. "Enough rubber volume" means large size, normally in proximity of 80 mm in diameter. "Enough rubber radial stiffness" indicates another major leaking factor: rubber aging. The aging of rubber results in the deterioration of its static stiffness, therefore the reliability of leaking worsens. Those two problems, inflexibility in size and poor reliability in leaking, become major concerns about the maturity of the existing hydrobushing technology. This paper proposes a hydrobushing design whose inertia track is placed outside of an aluminum armature which makes the inertia track independent to the main rubber element (Fig.3). As a result, the tri-axis static stiffness of the bushing is able to be

ISBN: 978-988-19251-5-2
ISSN: 2078-0958 (Print); ISSN: 2078-0966 (Online)

designed the same way as the conventional rubber bushing's. Therefore the design posses the flexibility in size selection. A thin layer of rubber is coated outside of the armature, and it is compressed tightly when the outer can is swaged. As a result, a reliable way to prevent the leaking is formed.

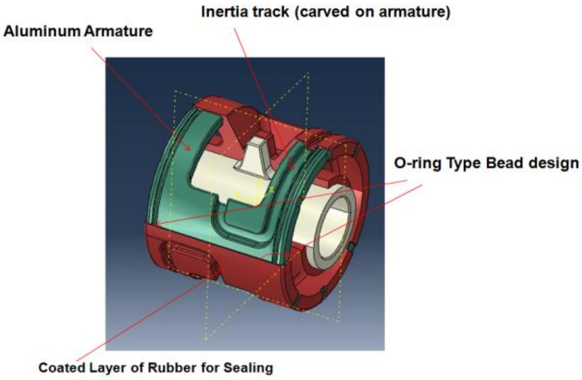


Figure 3: Proposed Hydrobushing Model

## II. Design Procedure

To illustrate the design process, an assumed design criterion is made (Table 1). The steps from the size determination, rate calculation, and performance prediction, which lead to the final design, are introduced. The suitable durability test device and setup is also discussed.

Table 1: A Set of Assumed Design Criterion

| Size | Crushing | Rate | Performance | Durability |
|---|---|---|---|---|
| Max. OD = 80 mm Min. ID = 22 mm Max. L = 75 mm Max. travel 8 mm | The inner tube is not allowed to exceed 0.4% of permanent deformation under 150 KN axial load | Axial (220) N/mm REF Void 350 ±15% N/mm Solid 1000 N/mm | 60 degree loss angle at 19 (±3) Hz | -No leak for B10-200,000 cycles -Rate change<25 % |

### A. Size Determination

Design criterion states that the minimum ID is 22 mm, so let the inner tube ID be 22 mm. Choose the material for the inner tube as hot rolled ANSI 1010/1008 steel, at which the yield stress is 180 MPa, ultimate stress 325 MPa, and elongation 28%.

The requirement for less than 4% of permanent deformation under the 150 KN crushing load is met by

$$\frac{Crushing\ Load}{Tube\ Cross\ section\ Area} = \sigma_y \qquad (1)$$

where the material is still in the elastic region. Therefore, the wall thickness of inner tube is 4 mm for the crushing load of 150 KN.

Therefore, the ID of the main rubber element must be 30 mm. The OD of the main rubber element is flexible. The decision is to try at 52 mm.

The aluminum armature will be molded into the outside of the main rubber element. Considering the carved inertia track on the armature, the wall thickness of the armature is assumed to be 4.5 mm. The outer can uses a 2 mm thick steel tube. Therefore, the OD of the hydrobushing is 65 mm.

The length of hydrobushing is flexible as well. The choice in this design is 60 mm for the inner tube, and 55 mm for the main rubber element.

The proposed design dimensions are summarized in Table 2.

Table 2: Proposed Design Dimensions

| | |
|---|---|
| 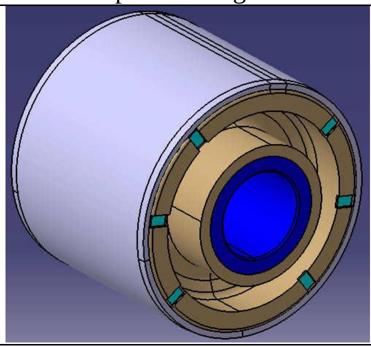 | ID: 22 mm<br>OD: 65 mm<br>Inner tube length: 60 mm<br>MRE length: 55 mm |

### B. Stiffness Prediction Using FEA

To determine if the proposed dimensions can meet the tri-axis rate requirements, commercially available FEA software, ABAQUS, is employed. Duro 55 natural rubber, whose hardness is in proximity of the application, is used. The material model is chosen to be the second order polynomial of the strain energy function, whose material coefficients are $C_{10}$=0.3517 MPa, and $C_{01}$=0.09266. Fig. 4 illustrates the effort in searching the geometry of the main rubber element: from a very simple one to the design whose rates meets the requirements through many iterations.

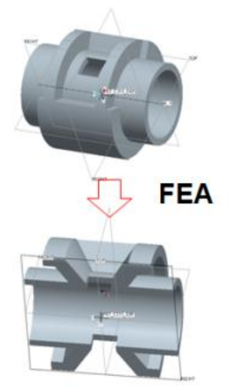


Figure 4: Design iterations

Once the geometry of the main rubber element is found, the aluminum armature with its ID of 53 mm and wall thickness of 4.5 mm is added. The armature has no significant impact on rates due to the fact that the main

ISBN: 978-988-19251-5-2
ISSN: 2078-0958 (Print); ISSN: 2078-0966 (Online)

rubber element is independent to it. The rate results from FEA are shown in Fig.5, 6 and 7.

Table 3 lists the comparison of the predicted rates versus targeted.

Table 3: Summary of FEA Rate Prediction

| Direction | Target Rate (N/mm) | Predicted Rate (N/mm) | % of Error |
|---|---|---|---|
| Solid | 1000 | 1072 | 7.2 |
| Void | 350±15% | 355 | 1.4 |
| Axial | (220) REF | 243 | 10.5 |

### C. *Performance Prediction*

The mathematical model of the hydrobushing is shown in Fig.8 [5], at which $\boldsymbol{k}_s$ is main rubber element static stiffness in the fluid chamber direction; $\boldsymbol{k}_v$ is volumetric stiffness (additional stiffness in the fluid chamber direction caused by the incompressible flow). The fluid density is $\boldsymbol{\rho}$, inertia track length is $\boldsymbol{L}$ and the inertia track cross section area is $a$. The projected area of the fluid chamber in the direction of motion is $\boldsymbol{A}$. Assume that the friction coefficient between the fluid and the inertia surface is $\boldsymbol{c}$. $\boldsymbol{C}_r$ is the rubber damping coefficient.

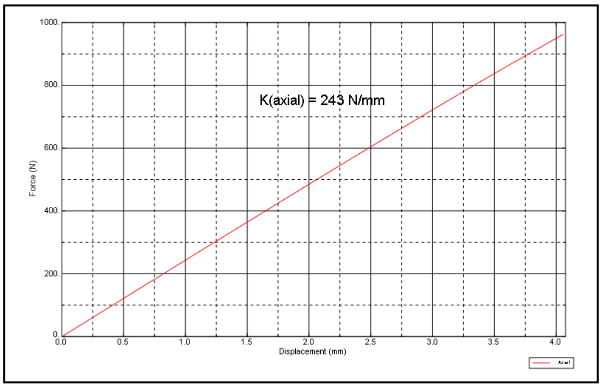


Figure 5: Predicted Axial Stiffness

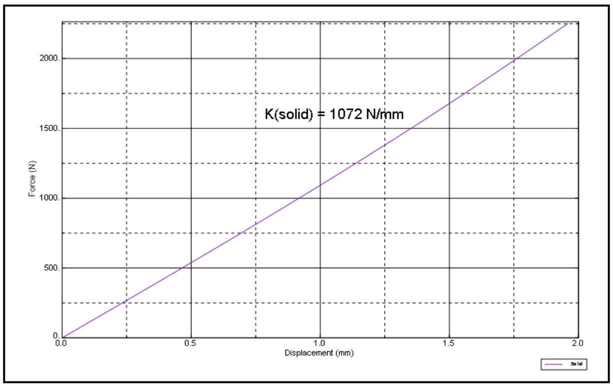


Figure 6: Predicted Radial Solid Stiffness

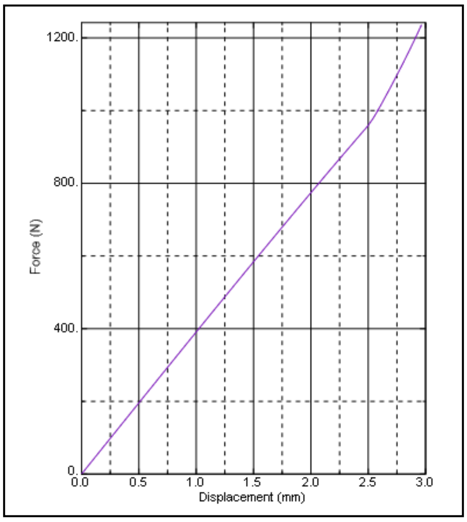


Figure 7: Predicted Radial Void Stiffness

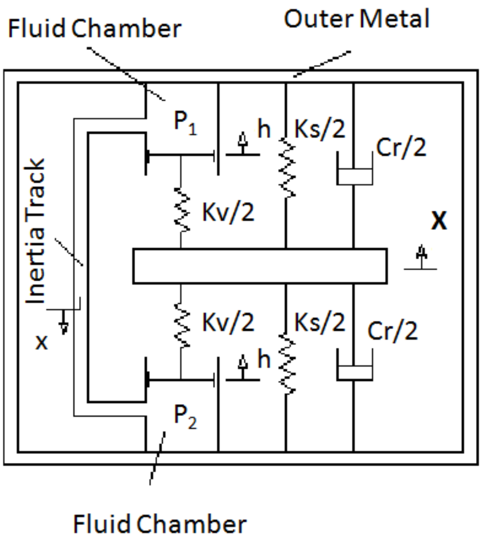


Figure 8: Hydrobushing Model

The dynamic properties of a hydrobushing, $\boldsymbol{K}$*, derived from this model according to Ref [5] is

$$k^* = k_s + k_v - \frac{k_v^{\,2}\left(\frac{a}{A}\right)^2}{k_v\left(\frac{a}{A}\right)^2 - la\rho\omega^2 + ic\omega} \tag{2}$$

The magnitude of dynamic stiffness is

$$k_d = \sqrt{k'^2 + k''^2} \tag{3}$$

and the loss angle φ is

$$\varphi = \tan^{-1}\frac{k''}{k'} \tag{4}$$

ISBN: 978-988-19251-5-2
ISSN: 2078-0958 (Print); ISSN: 2078-0966 (Online)

where k' and k" are real and imaginary parts of Eq.2.

The maximum damping occurs when the fluid in the inertia track resonates:

$$f = \frac{1}{2\pi}\sqrt{\frac{k_v\left(\frac{a}{A}\right)^2}{la\rho}} \tag{5}$$

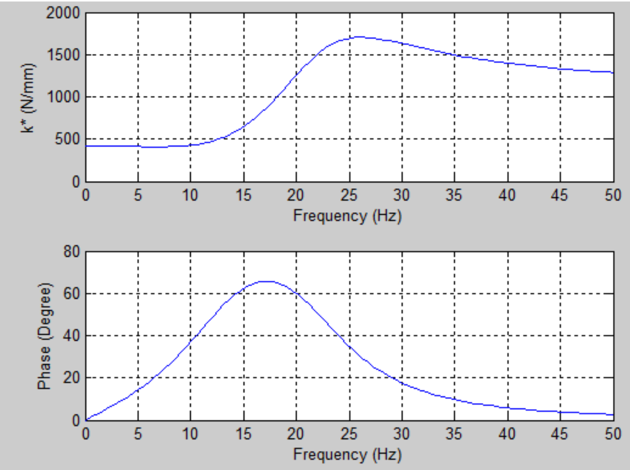


ng

Figure 9: Predicted Dynamic Properties of Hydrobushing

The predicted dynamic properties of the hydrobushing shown in Fig.9 are based on a set of variables in Table 4, at where the friction coefficient of fluid and the volumetric stiffness are estimations. Matlab is the computing software which is used.

Table 4: Variables Meeting the Performance Criterion

| $K_s$ | **Kv** | **l** | **a** | **A** | **c** | **ρ** |
|---|---|---|---|---|---|---|
| 350 N/mm | 700 N/mm | 250 mm | 9 $mm^2$ | 1100 $mm^2$ | 0.25 Ns/m | 1000 $kg/m^3$ |

It is seen that the frequency at the maximum loss angle is apporximately 17 Hz, which is in the range of 19 Hz±3. The maximum phase angle is around 65 degrees.

## *D. Component Design*

*Armature*

The overall dimensions of the armature, ID of 52 mm and wall thickness of 4.5 mm, were decided earlier. The inertia track with the cross sectional area of 9 $mm^2$ and the length of 250 mm is carved out from the outside of the armature based on the performance analysis outcome. To prevent the fluid leaking through the sides, two identical grooves with a 1 mm radius are cut out in each side of the armature so that the filled rubber serves as o-rings for seal (Fig.10). The finished design model is shown in Fig.11. The material for this component is A380.

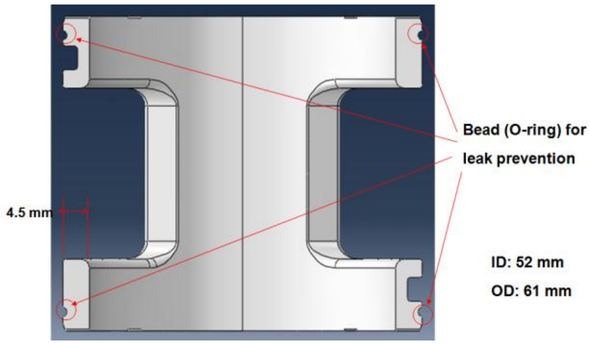


Figure 10: O-ring Groove Design

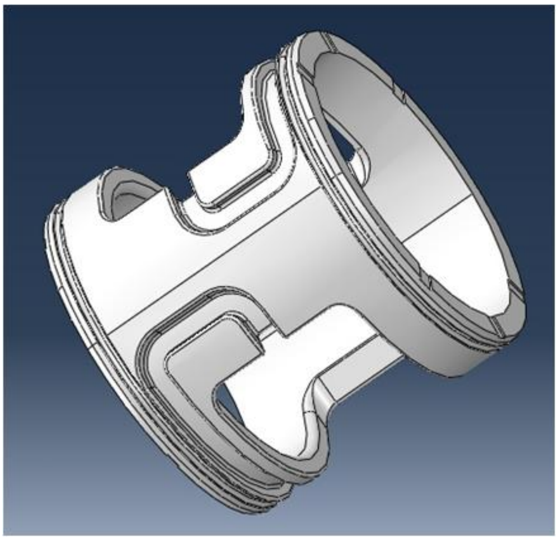

Figure 11: Isometric Model of Armature Design

*Inner Tube and Travel Limit*

The inner tube dimension and its material were determined earlier. The new feature for the inner tube design in this stage is to add the travel limits (Fig. 12). The damping is needed in the initial few millimeters of displacement. Further displacement is controlled by the travel limit, when metal to metal contact between the travel limit and the outer can inner surface occurs. The travel limit is made from AISI 1010/1008 steel and is welded in the middle of the inner tube.

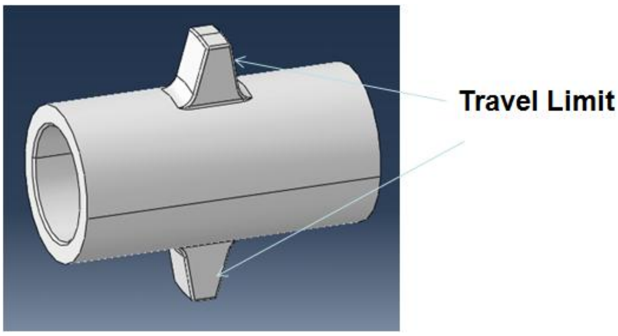


Figure 12: Inner Tube Design

ISBN: 978-988-19251-5-2
ISSN: 2078-0958 (Print); ISSN: 2078-0966 (Online)

*Outer Can*

The outer can is a 2 mm thick steel tube. Its material is AISI 1010/1008. The OD and ID in the assembled state are 65 mm and 61 mm respectively. Due to the need for the swaging process, the pre-assembled dimensions for OD and ID are 66 mm and 62 mm. The swaging process reduces the outer can OD by 1 mm, which is enough to compress the 0.5 mm thick coated rubber in the outside of the armature for sealing purposes. The solid model of the outer can design is shown in Fig.13.

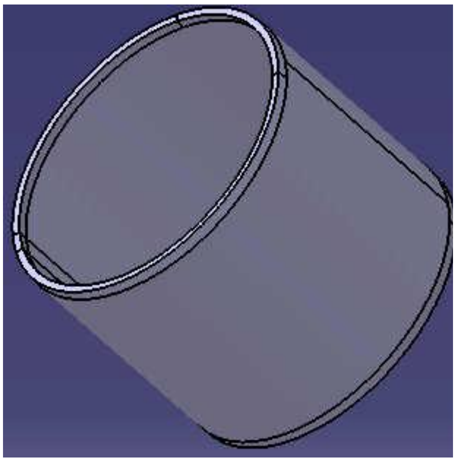

Figure 13: Outer Can Model

### E. *Durability Test*

The approach to verify if the design meets the durability requirement is to build a prototype and test it. Fig.14 illustrates the required loadings in the test setup. The example of the suitable test equipment, MTS Tri-axis dynamic tester, is shown in Fig.15.

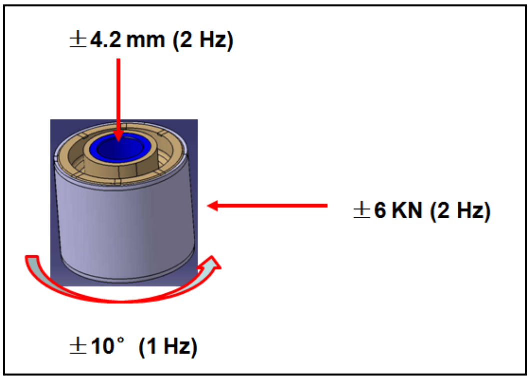


Figure 14: Durability Loading Setup

## III. Conclusion

An improved design of the automotive hydraulic bushing features an added aluminum armature whose inertia track is carved outside is presented. The inertia track is independent to the main rubber element, therefore the requirement of tri-axis rates is met by the same design process as conventional rubber bushing, which makes the design as size flexible. The coated rubber in the outside of the armature serves as the tight seal as it is compressed in the assembly process when the outer can is swaged. The O-ring feature on both side of the armature reinforce the sealing capability. Therefore, the design improves the reliability in leak prevention.

Figure 15: MTS Tri-axis Tester

| Maker | MTS |
|---|---|
| Spec. | Load: ±25 KN<br>Disp: ±35 mm<br>Torsional angle: ±10°<br>Frequency: 0-80 Hz<br>Temperature: -50-100°C |

## References

[1] Muzechuk, R.H, Hydraulic Mounts-Improved Engine Isolation, SAE Paper 840410..
[2] Bernuchon, M., A New Generation of Engine Mounts, SAE Paper 840259.
[3] Flower, W.C., Understanding Hydraulic Mounts for Improved Vehicle Noise, SAE Paper 850975.
[4] Clark, M., Hydraulic Engine Mount Isolation, SAE Paper 851650.
[5] Lu,M. and Ari-Gur, J., Study of Dynamic Properties of Automotive Hydrobushing, Proceeding of IMECE, 2000 ASME International Congress and Exposition, Nov 5-10, Orlando, Florida, USA.

ISBN: 978-988-19251-5-2
ISSN: 2078-0958 (Print); ISSN: 2078-0966 (Online)